

**Figure S1. Association of *Terc-53* with Alzheimer's disease.**

(A) Northern blotting examination of *Terc-53*, and full-length *Terc* in N2a and N2a-APP695 cells. 5S rRNA was used as a loading control.

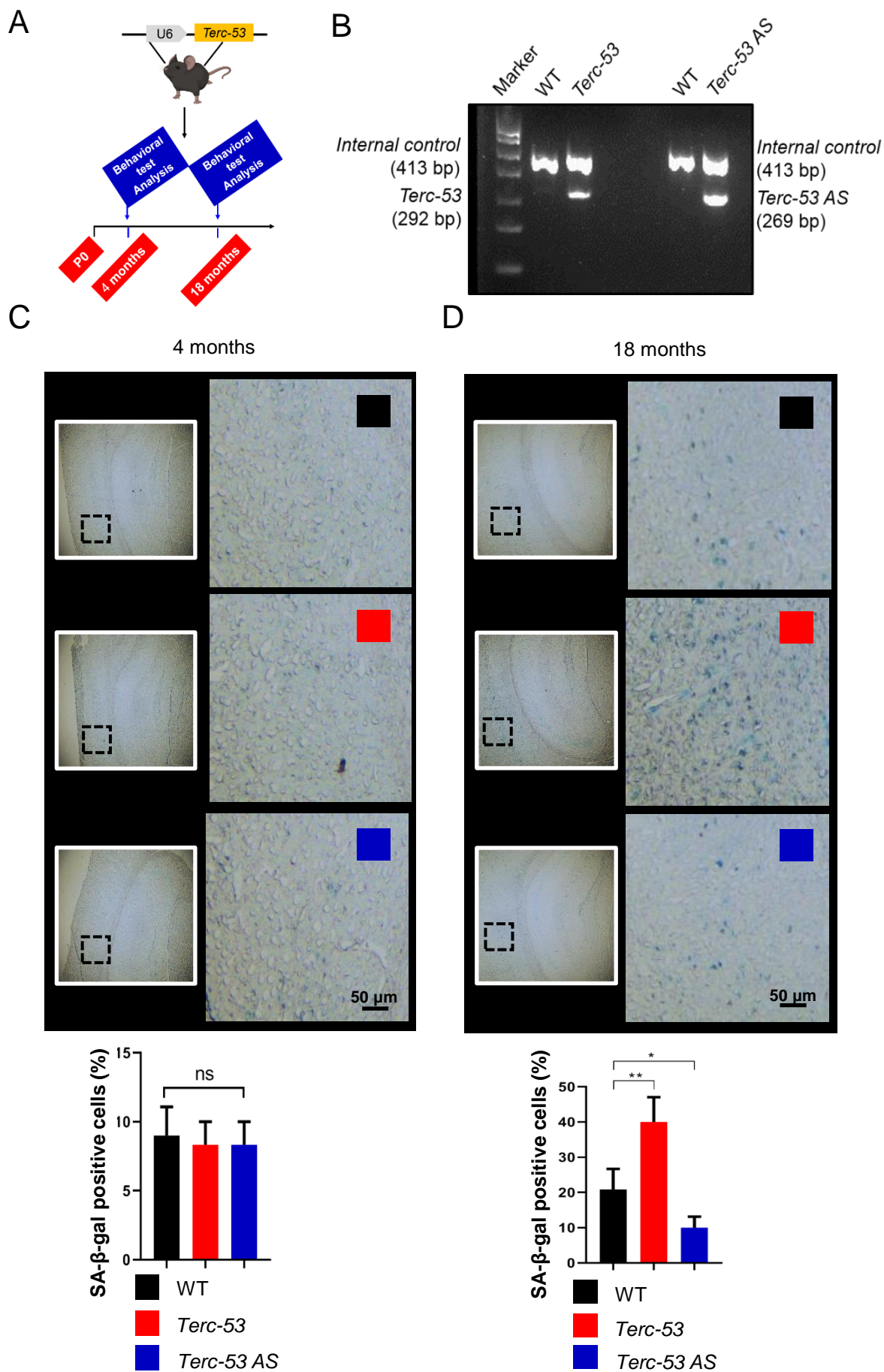
(B) Quantification of the relative *Terc-53* levels in Panel A (n = 3).

(C) Genotyping of day 21 WT and 5× FAD mice.

(D) Northern blotting examination of *Terc-53* and full-length *Terc* in the hippocampus of 5× FAD male mice and wild-type (WT) male mice at 6 months of age. 5S rRNA was used as a loading control.

(E) Quantification of the relative *Terc-53* levels in Panel D (n = 3).

Data are presented as Mean  $\pm$  SD. ns, no significance, \*p < 0.05, \*\*p < 0.01.



E

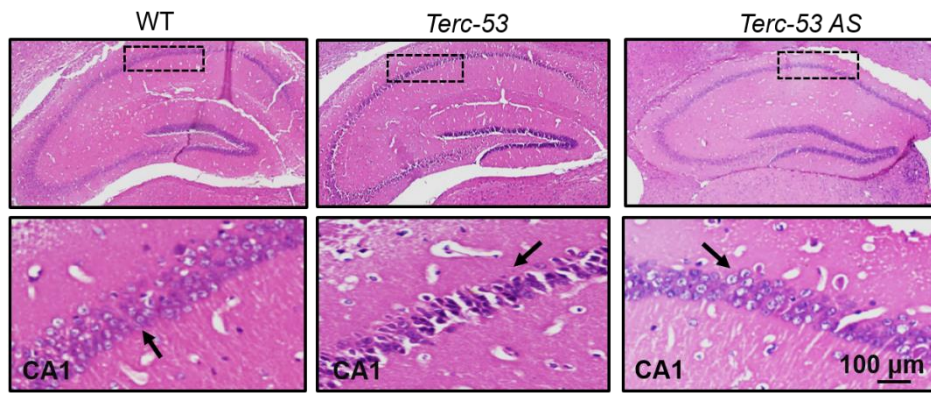


**Figure S2. *Terc-53* overexpression causes abnormality in the 18-month-old mouse hippocampus.**

(A) Schematic of the strategy for generating the transgenic *Terc-53*-overexpressing mice (*Terc-53*) and transgenic *Terc-53* antisense-expressing mice (*Terc-53 AS*) and the time point experimental flowchart.

(B) Genotyping of 21-day-old WT, *Terc-53* and *Terc-53 AS* mice using PCR. The higher band is an internal PCR control.

(C) Representative SA- $\beta$ -gal staining images of the brain sections of WT, *Terc-53* and *Terc-53 AS* male mice at 4 months of age (top panels), and quantification of the SA- $\beta$ -gal positive cells (bottom panel).

(D) Representative SA- $\beta$ -gal staining images of the brain sections of WT, *Terc-53* and *Terc-53 AS* male mice at 18 months of age (top panels), and quantification of the SA- $\beta$ -gal positive cells (bottom panel).

(E) Representative hematoxylin and eosin (H&E) staining images of the brain sections of WT, *Terc-53* and *Terc-53 AS* mice at 18 months of age. The nucleus shows in purple while the cytoplasm shows in red. Black arrows indicate the neurons.

Data are presented as Mean  $\pm$  SD. ns, no significance, \* $p < 0.05$ , \*\* $p < 0.01$ .

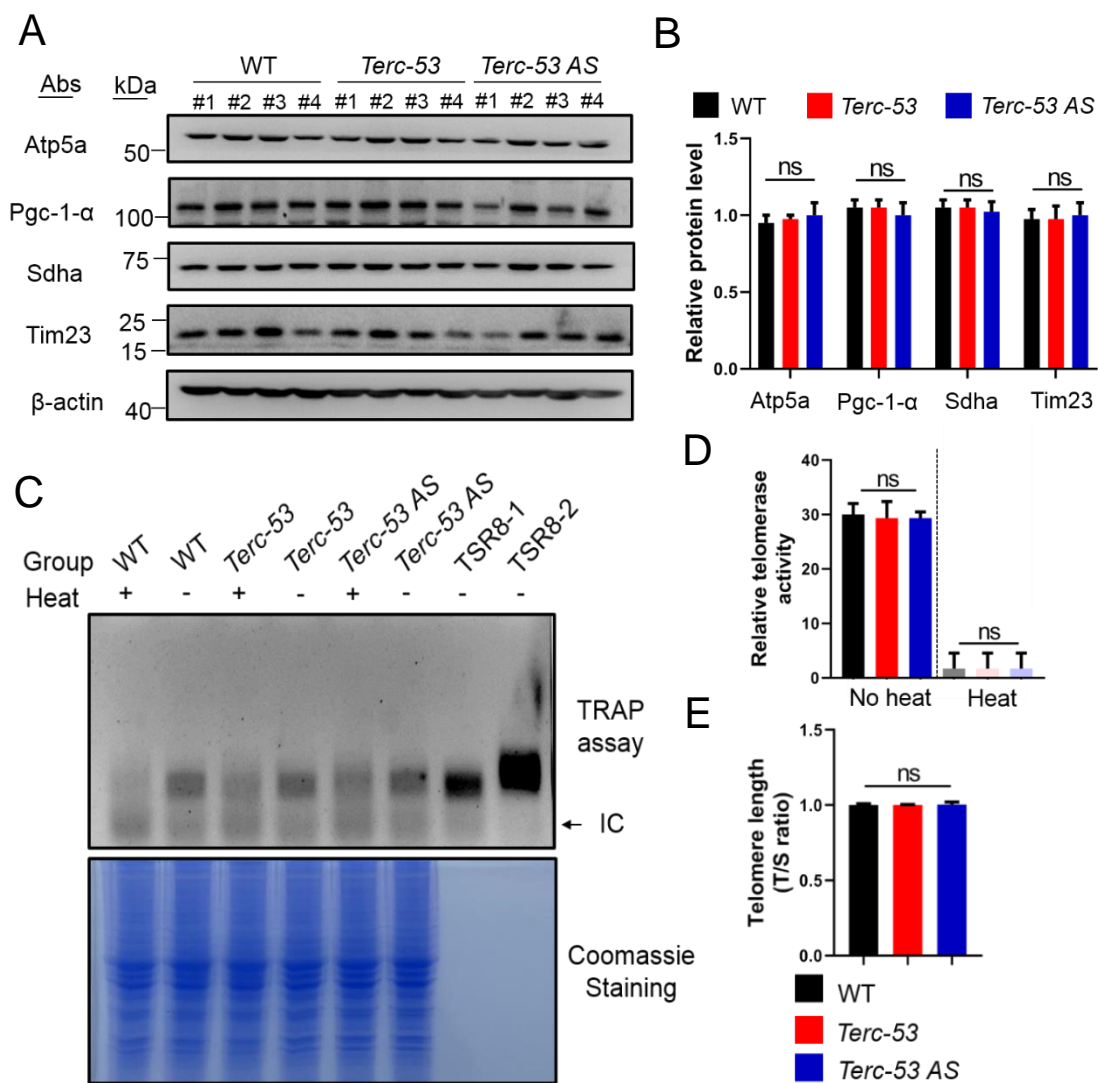


**Figure S3. *Terc-53* overexpression does not affect mitochondrial biosynthesis and functions or telomerase activity.**

(A) Immunoblots of the proteins that are involved in mitochondrial biosynthesis and functions in the hippocampus of the three groups of mice at 18 months of age.  $\beta$ -actin was used as a loading control.

(B) Quantification of the relative protein levels in Panel A.

(C) Measurement of telomerase activity in the hippocampus of the three groups of mice at 18 months of age by telomerase repeat amplification protocol (TRAP) assay. The bottom panel is a Coomassie staining gel of the hippocampus lysates as the loading control.

(D) Quantification of the relative telomerase activity in Panel C (n = 3).

(E) Measurement of the telomere length in the cortex of the three groups of mice at 18 months of age, using a real-time qPCR method and calculating telomere PCR (T) /single copy gene PCR (S) ratio.

Data are presented as Mean  $\pm$  SEM. ns, no significance.

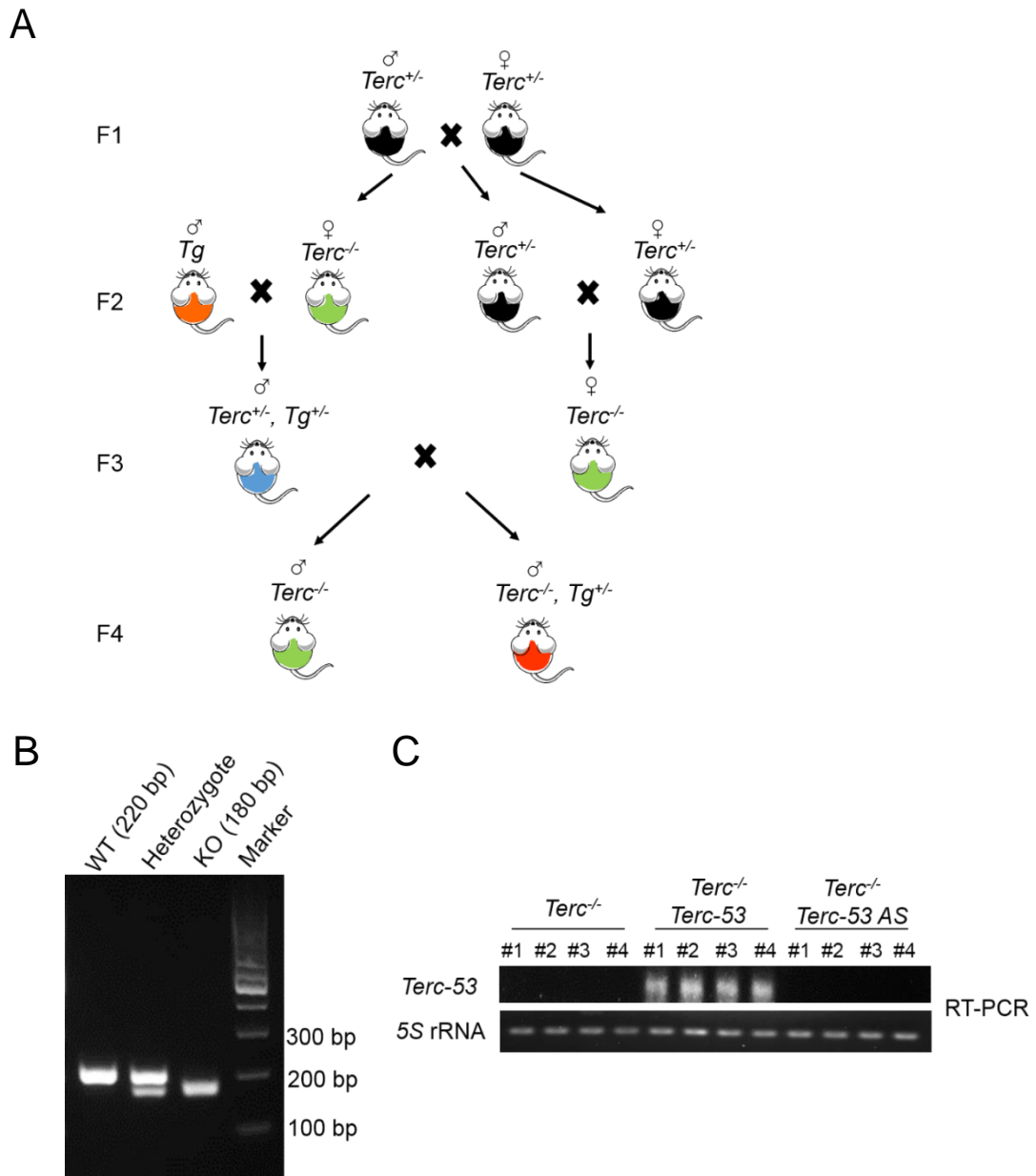
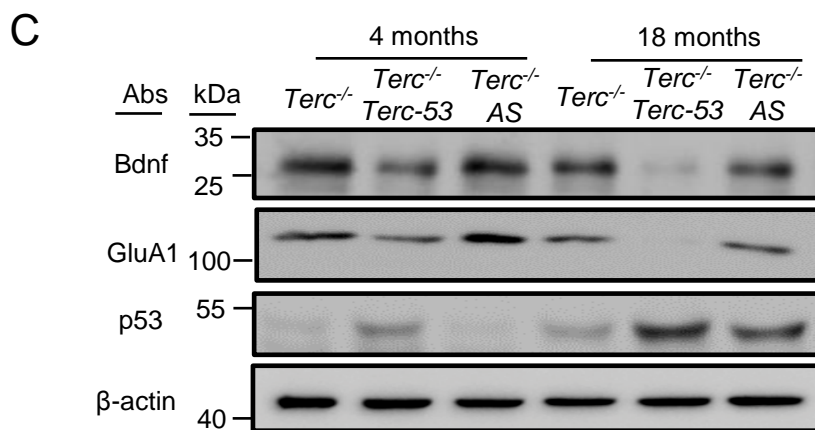
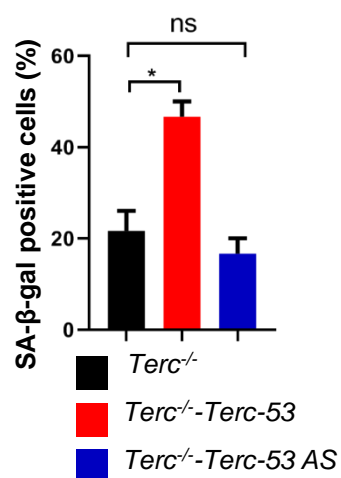
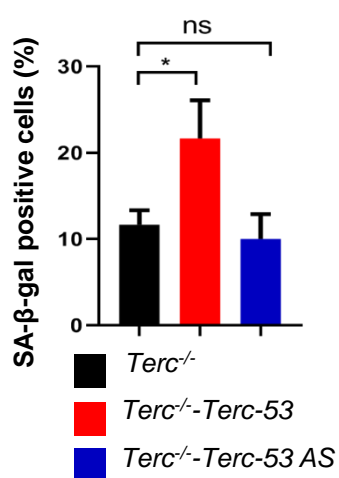
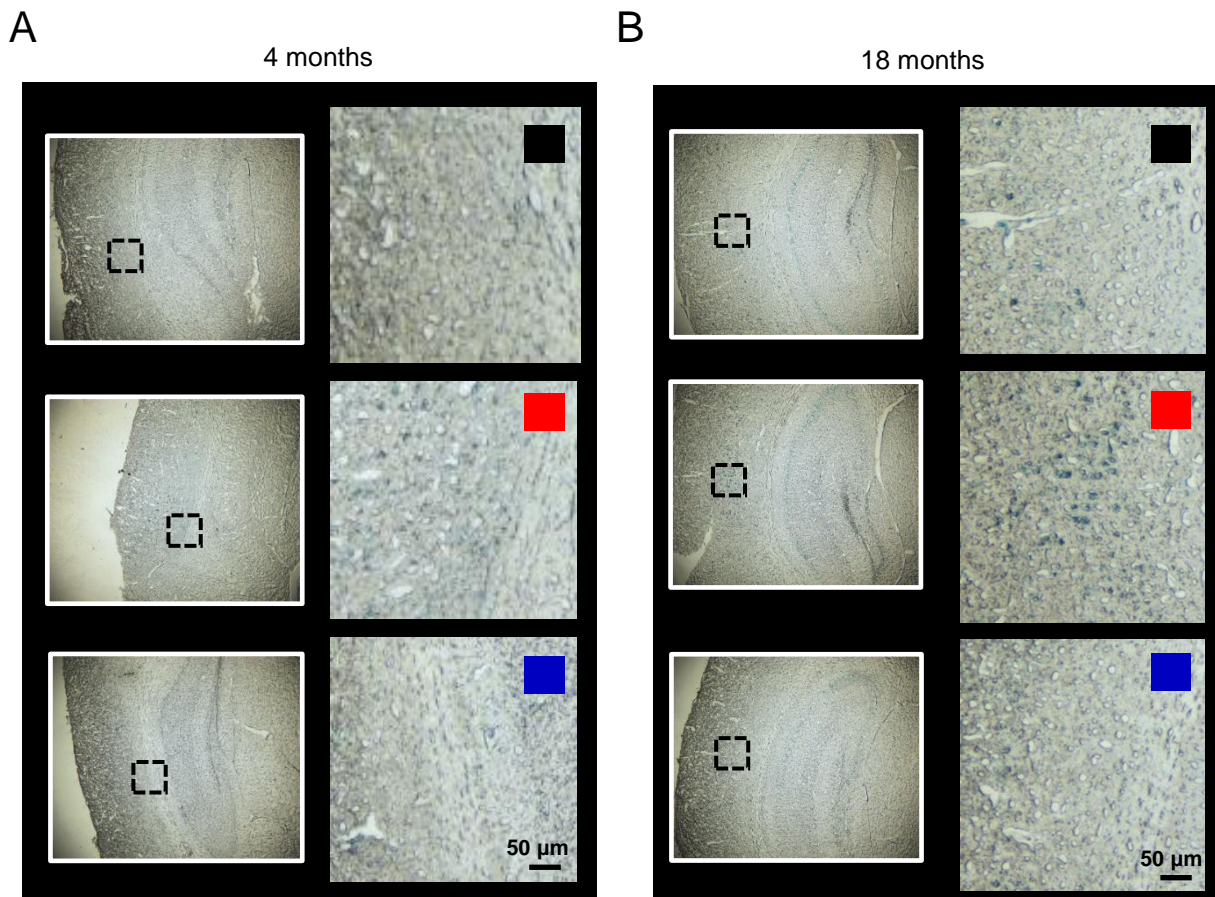


**Figure S4. Generation of *Terc*-53 transgenic mice on *Terc*<sup>-/-</sup> background.**

(A) Schematic of the strategy for generating the *Terc* knockout (*Terc*<sup>-/-</sup>), *Terc* knockout plus transgenic *Terc*-53-overexpressing mice (*Terc*<sup>-/-</sup>-*Terc*-53), and *Terc* knockout plus transgenic *Terc*-53 antisense-expressing mice (*Terc*<sup>-/-</sup>-*Terc*-53 AS).

(B) Genotyping of 21-day-old WT, *Terc*<sup>+/-</sup> and *Terc*<sup>-/-</sup> mice.

(C) *Terc*-53 levels in the cortex of *Terc*<sup>-/-</sup>, *Terc*<sup>-/-</sup>-*Terc*-53 and *Terc*<sup>-/-</sup>-*Terc*-53 AS mice at 18 months of age were examined using RT-PCR. 5S rRNA was used as a loading control.



D

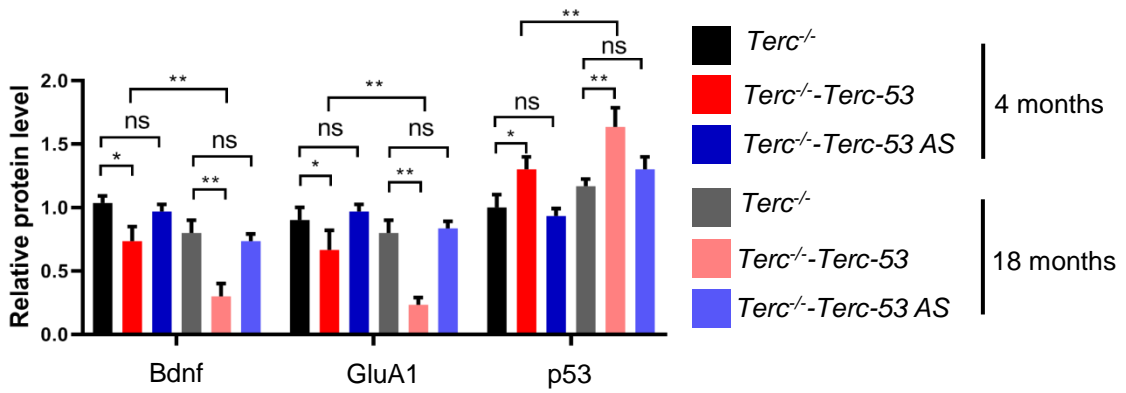


**Figure S5. The effects of *Terc*-53 overexpression on ageing markers in the hippocampus of *Terc*<sup>-/-</sup> mice.**

(A) Representative SA- $\beta$ -gal staining images of the brain sections of *Terc*<sup>-/-</sup>, *Terc*<sup>-/-</sup>-*Terc*-53 and *Terc*<sup>-/-</sup>-*Terc*-53 AS male mice at 4 months of age (top panels), and quantification of the SA- $\beta$ -gal positive cells (bottom panel).

(B) Representative SA- $\beta$ -gal staining images of the brain sections of *Terc*<sup>-/-</sup>, *Terc*<sup>-/-</sup>-*Terc*-53 and *Terc*<sup>-/-</sup>-*Terc*-53 AS male mice at 18 months of age (top panels), and quantification of the SA- $\beta$ -gal positive cells (bottom panel).

(C) Immunoblots of Bdnf (Brain-derived neurotrophic factor) and GluA1 (an AMPA receptor subunit) in the hippocampus of the three groups of mice at 4 and 18 months of age.  $\beta$ -actin was used as a loading control.

(D) Quantification of the relative protein levels in Panel C (n = 4).

Data are presented as Mean  $\pm$  SD. ns, no significance, \*p < 0.05, \*\*p < 0.01.

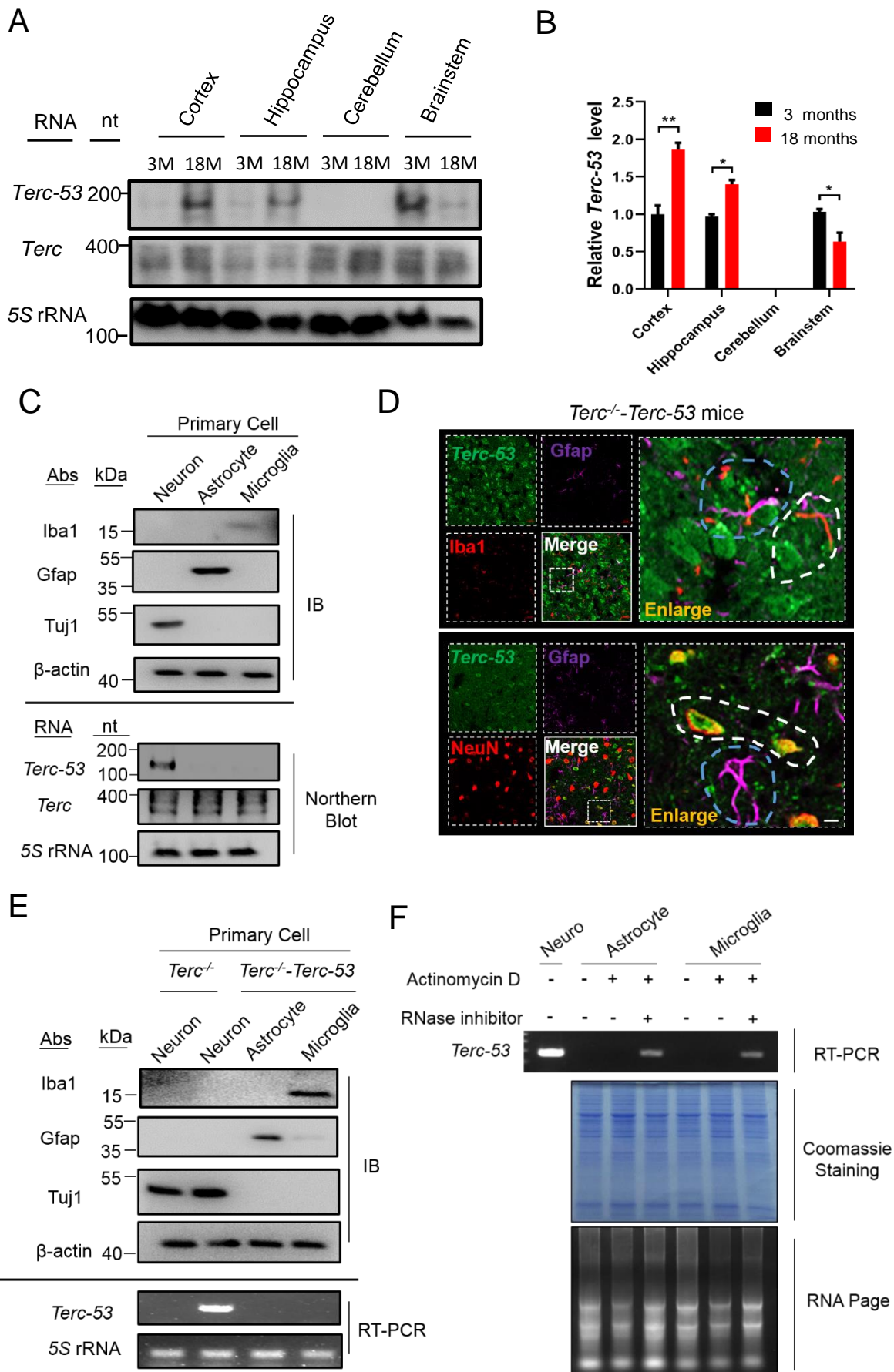


**Figure S6. *Terc-53* is specifically expressed in neurons.**

(A) *Terc-53* and full-length *Terc* expression levels in different brain regions of 3-month-old and 18-month-old wild-type male mice were examined by Northern blotting. 5S rRNA was used as a loading control.

(B) Quantification of the relative *Terc-53* levels in Panel A (n = 4).

(C) Top panels: isolation of primary cells from 3-month-old wild-type mice and verification of their identities using specific markers (neuron: Tuj1; astrocyte: Gfap; microglia: Iba1).  $\beta$ -actin was used as a loading control. Bottom panels: Northern blotting examination of *Terc-53* and full-length *Terc* levels in these primary cells. 5S rRNA was used as a loading control.

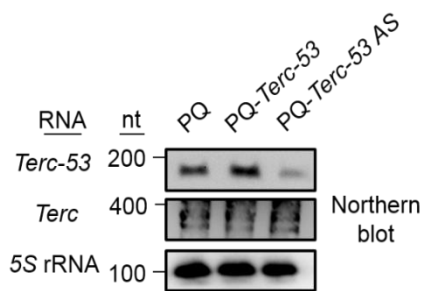
(D) Fluorescence in situ hybridization (FISH) examination of *Terc-53* and immunofluorescence staining of Iba1, Gfap and NeuN in the hippocampus of 6-month-old *Terc*<sup>-/-</sup>-*Terc-53* mice.

(E) Top panels: isolation of primary cells from 6-month-old *Terc*<sup>-/-</sup> and *Terc*<sup>-/-</sup>-*Terc-53* mice and verification of their identities using specific markers (neuron: Tuj1; astrocyte: Gfap; microglia: Iba1).  $\beta$ -actin was used as a loading control. Bottom panels: RT-PCR examination of *Terc-53* levels in these primary cells. 5S rRNA was used as a loading control.

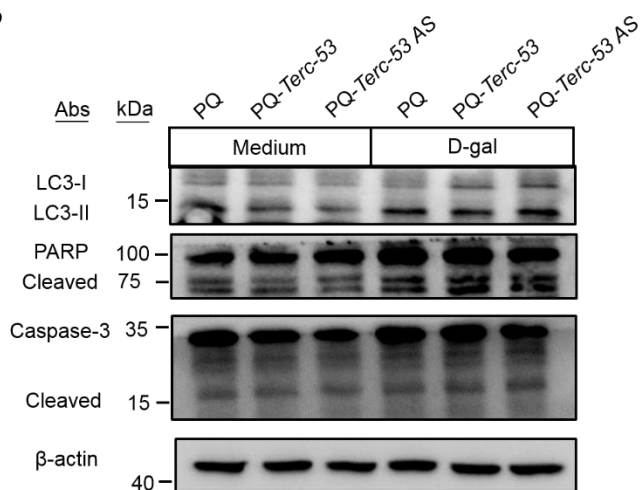
(F) RT-PCR examination of *Terc-53* levels in *Terc*<sup>-/-</sup>-*Terc-53* primary neurons, astrocytes and microglia after actinomycin D (an transcription inhibitor) or/and RNase inhibitor treatment. The cells were treated with actinomycin D (10  $\mu$ g/ml) and RNase inhibitors (100 U/ml) for 2 h and 1 h, respectively. Bottom panels are a Coomassie staining gel as the loading control and an agarose gel of the total RNA as the inhibitor treatment control.

Data are presented as Mean  $\pm$  SD. ns, no significance, \*p < 0.05, \*\*p < 0.01.

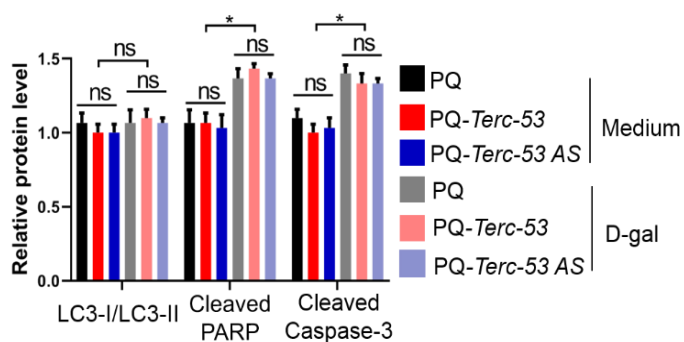
A



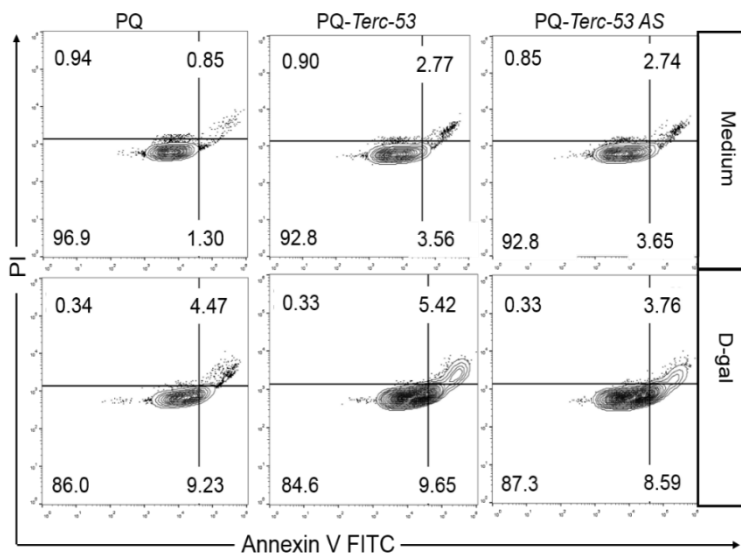
B



C



D



E

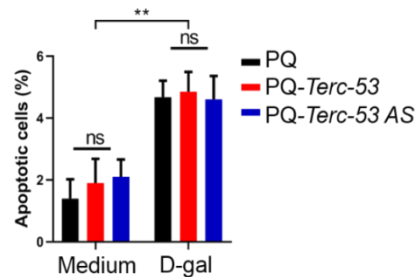


**Figure S7. *Terc-53* does not affect autophagy or apoptosis of N2a cells.**

(A) Northern blotting examination of *Terc-53* and full-length *Terc* levels in *Terc-53*-overexpressing (*Terc-53*), *Terc-53* antisense-expressing (*Terc-53 AS*), or the vector control (PQ) N2a cells. 5S rRNA was used as a loading control.

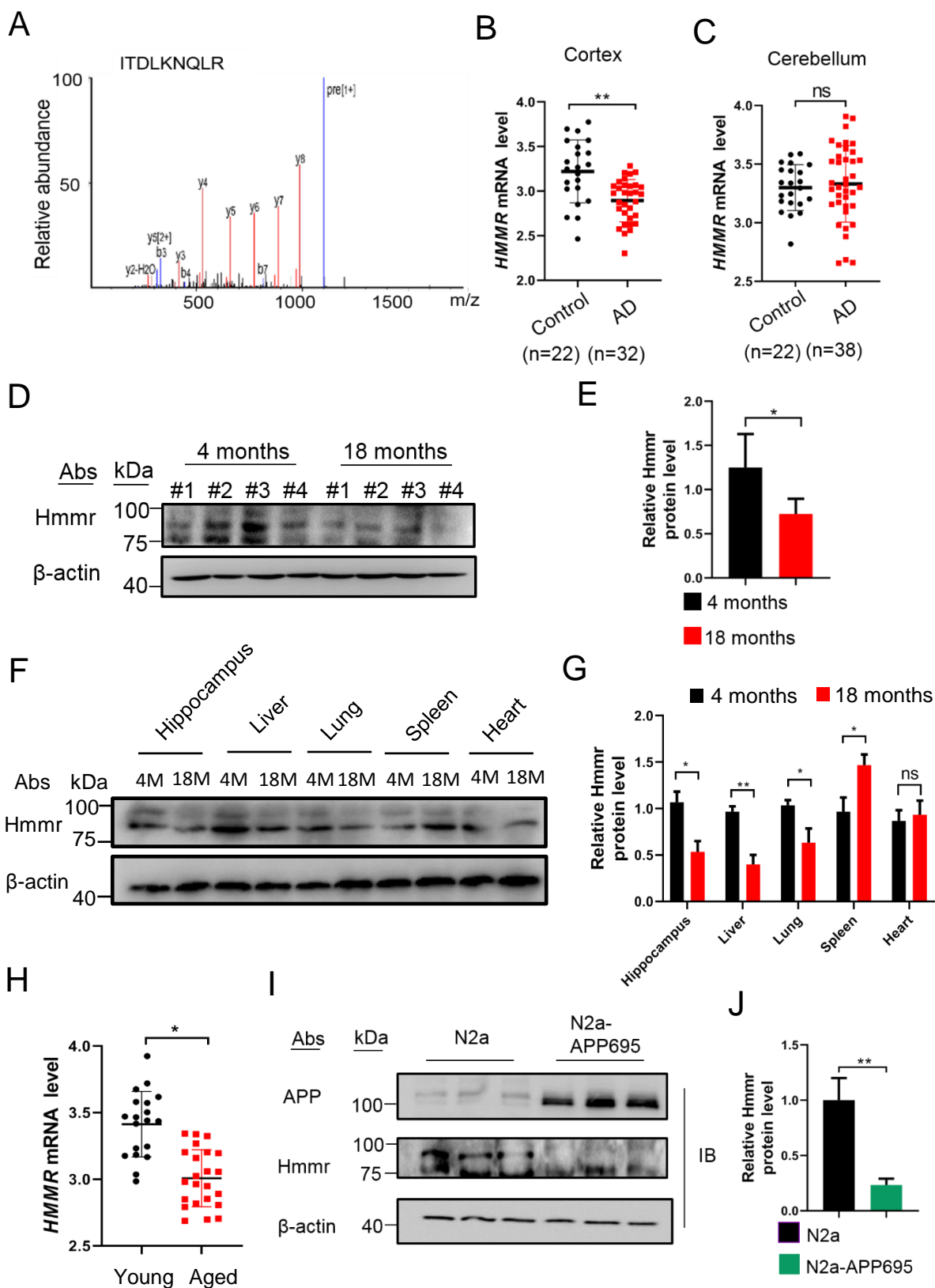
(B) Immunoblotting examination of LC3, cleaved-PARP, Caspase-3 and  $\beta$ -actin in *Terc-53*-overexpressing (*Terc-53*), *Terc-53* antisense-expressing (*Terc-53 AS*), or the vector control (PQ) N2a cells, with or without D-galactose (D-gal) treatment.

(C) Quantification of the relative protein levels in Panel B (n = 3).

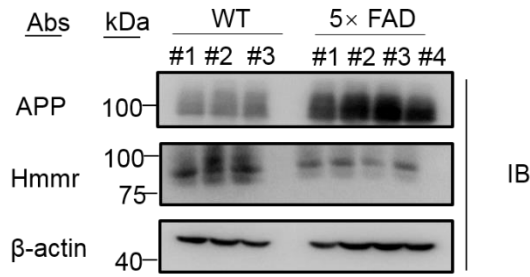
(D) Flow cytometry examination of apoptosis rates of *Terc-53*-overexpressing (*Terc-53*), *Terc-53* antisense-expressing (*Terc-53 AS*), or the vector control (PQ) N2a cells, with or without D-galactose (D-gal) treatment. FITC-conjugated Annexin V (AV)/PI double-staining was used to label the apoptotic cells.

(E) Quantification of apoptotic cells in Panel D (n = 3).

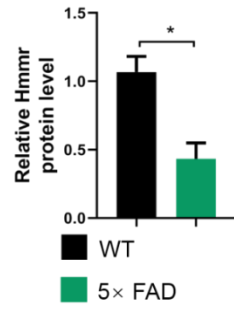
Data are presented as mean  $\pm$  SD. ns, no significance, \*p < 0.05, \*\*p < 0.01.



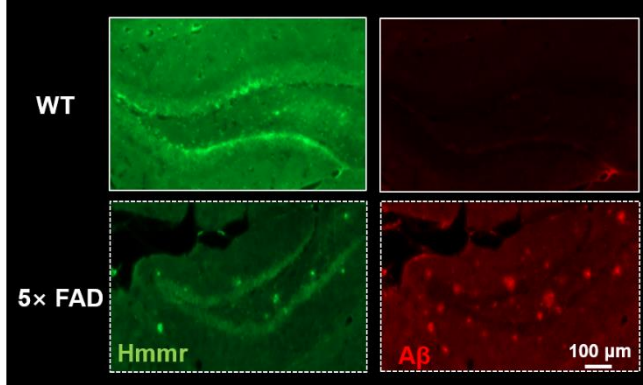
K



L



M



N

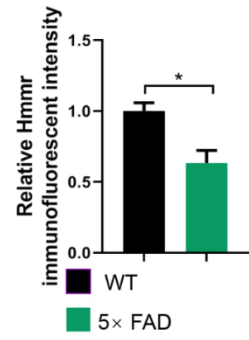


**Figure S8. Identification of Hmnr as a potential *Terc-53* effector.**

- (A) Mass spectrometry identification of Hmnr purified with the procedure shown in Fig. 2b.
- (B-C) *HMMR* expression in patients with Alzheimer's disease (AD) (n = 32) and unaffected controls (n = 22). Data from a tissue with AD neuropathology (cortex) and one partially spared by the disease (cerebellum) were analyzed. The sets of data were extracted from an existing database (Gene Expression Omnibus (GEO) accession number GSE118553).
- (D) Immunoblotting examination of Hmnr protein levels in the hippocampus of wild-type mice at 4 months and 18 months of age.
- (E) Quantification of the relative Hmnr protein levels in Panel D.
- (F) Immunoblotting examination of Hmnr protein levels in different tissues of wild-type male mice at 4 months and 18 months of age.  $\beta$ -actin were used as a loading control.
- (G) Quantification of the relative Hmnr protein levels in Panel F (n = 4).
- (H) *HMMR* expression levels in young and aged human brains (young < 60 years of age, n = 19; old > 60 years of age, n = 23), revealed by analyzing an existing RNAseq database (Gene Expression Omnibus (GEO) accession number GSE118553).
- (I) Immunoblotting examination of APP and Hmnr protein levels in N2a and N2a-APP695 cells.  $\beta$ -actin were used as a loading control.
- (J) Quantification of the relative Hmnr protein levels in Panel I (n = 3).
- (K) Immunoblotting examination of Hmnr and APP protein levels in the hippocampus of 5  $\times$  FAD male mice and wild-type (WT) male mice at 6 months of age.  $\beta$ -actin were used as a loading control.
- (L) Quantification of the relative Hmnr protein levels in Panel K (n = 3).
- (M) Immunofluorescent staining of Hmnr and A $\beta$  in the hippocampus of 6-month-old WT and 5  $\times$  FAD male mice.
- (N) Quantification of Hmnr protein levels in Panel M (n = 3).
- Data are presented as Mean  $\pm$  SD. ns, no significance, \*p < 0.05, \*\*p < 0.01



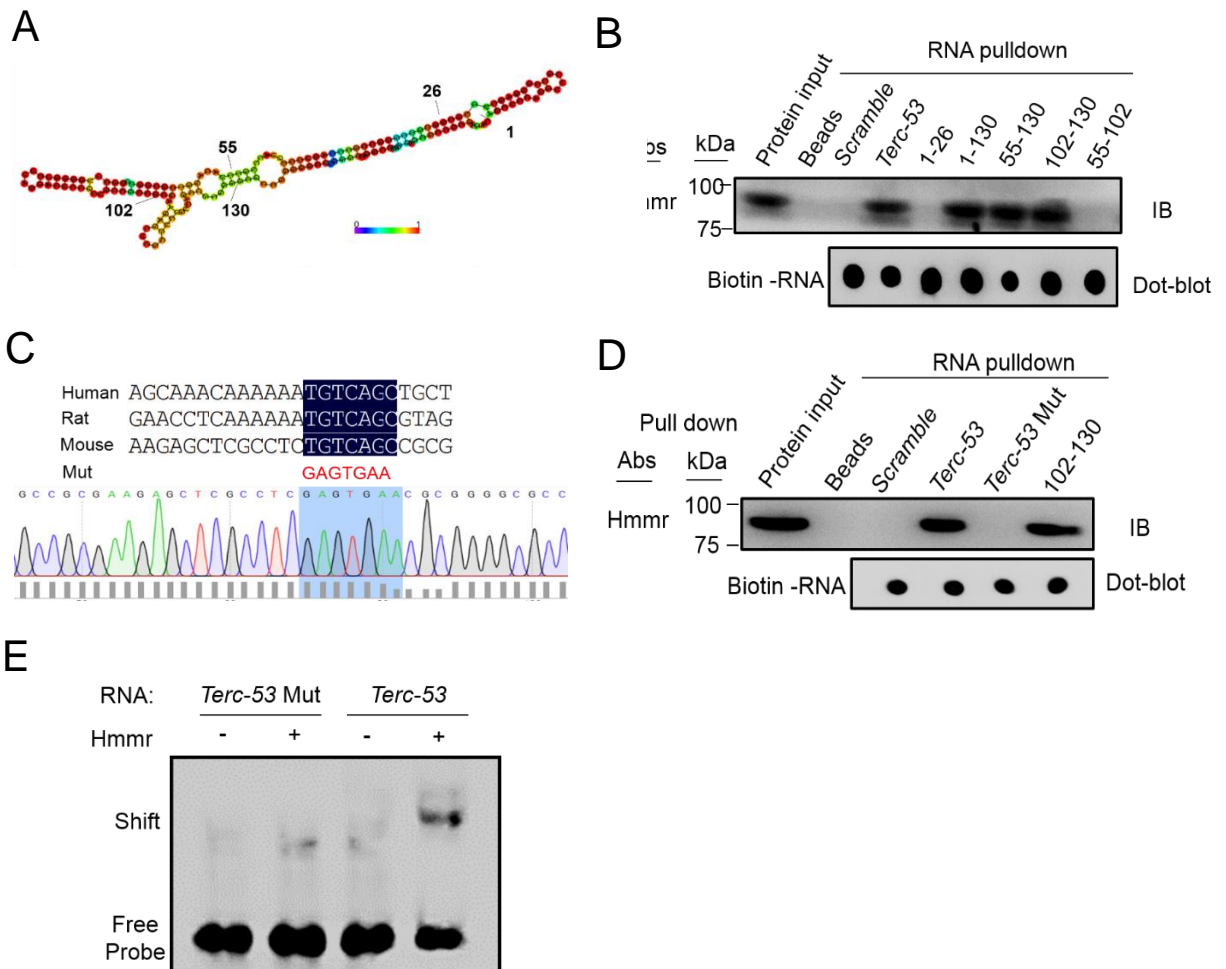


### Figure S10. Nucleotides 102-130 of *Terc-53* are involved in interaction with Hmnr.

(A) The predicted secondary structure of *Terc-53* by the Vienna RNA Package. The prediction was based on minimum free energy (MFE). Color scale indicates confidence of prediction for each base. Red shades indicate the predictions with strong confidence.

(B) In vitro RNA/protein interaction assay between biotin-labeled *Terc-53* of different lengths and purified His-Hmnr protein.

(C) The sequences of human, rat and mouse *Terc-53* (nt 102-130) with the most conserved region highlighted in black, and the changed nucleotides in mouse *Terc-53* mutant in red. The bottom panel shows the Sanger sequencing result, verifying the construction of the mutant.

(D) In vitro RNA/protein interaction assay between purified His-Hmnr protein, and the biotin-labeled RNAs as indicated. *Terc-53* and *Terc-53* 102-130 were used as positive controls.

(E) Gel shift assay of biotin-labeled *Terc-53* or *Terc-53* Mutant with purified His-Hmnr protein.

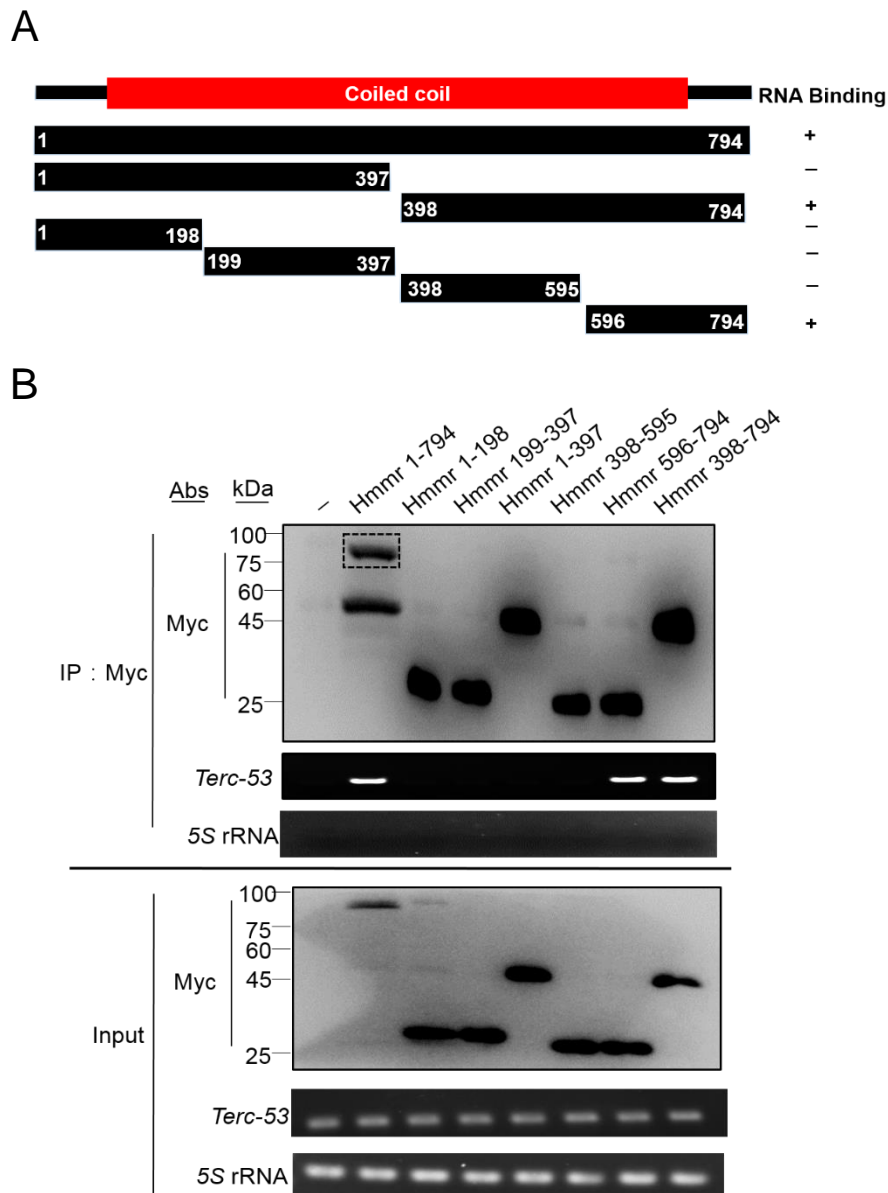
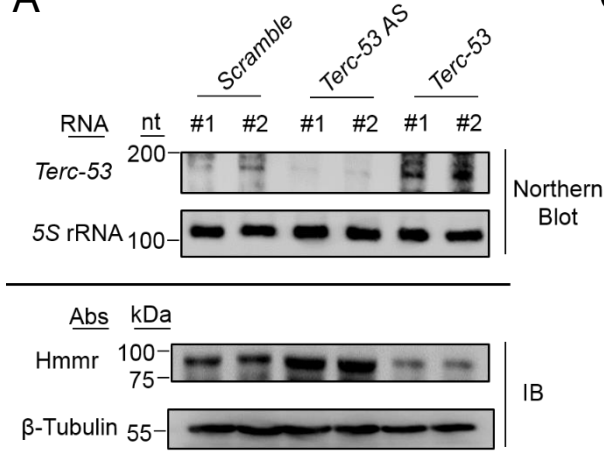


**Figure S11. The C-terminus (amino acids 596-794) of Hmnr is involved in interaction with *Terc-53*.**

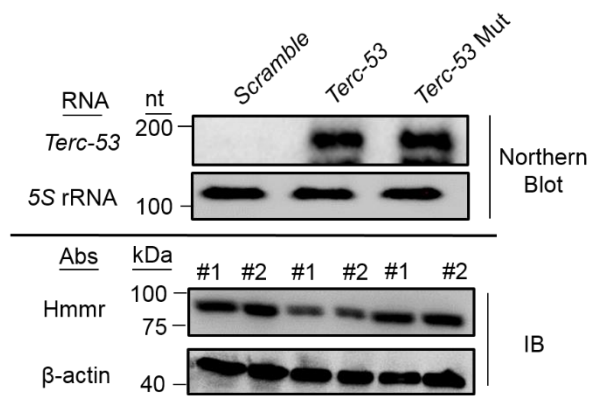
(A) Schematic of Hmnr and different truncations.

(B) N2a cells were transfected with full-length or truncation constructs of Myc-Hmnr for 2 days. Hmnr complexes were immuno-precipitated using Myc magnetic beads, and examined by immunoblotting using anti-Myc antibody. The box of dashed line indicates the band of the correct size of Hmnr 1-794. The levels of co-purified *Terc-53* were determined by RT-PCR.

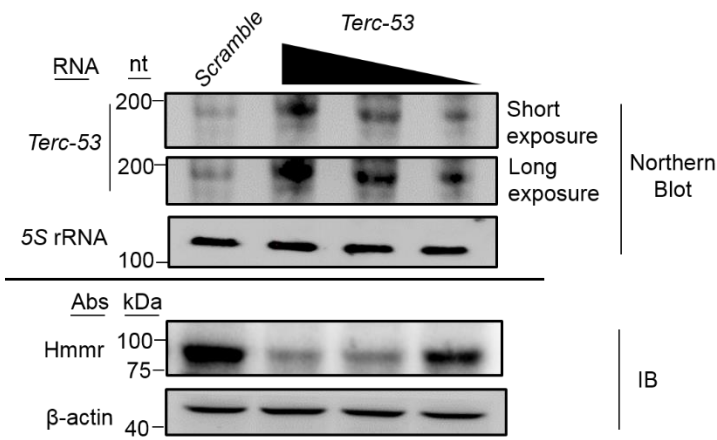
**A**



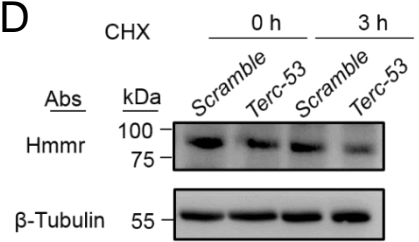
**C**



**B**



**D**



**E**

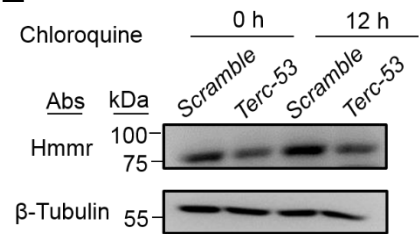


**Figure S12. *Terc-53* regulates Hmnr protein stability.**

(A) Northern blotting examination of *Terc-53* levels (Top) and immunoblotting examination of Hmnr protein levels (Bottom) in N2a cells stably expressing *Terc-53*, *Terc-53 AS* or the *Scramble* RNA. 5S rRNA and  $\beta$ -tubulin were used as loading controls.

(B) Immunoblotting examination of Hmnr protein levels (bottom panels) in N2a cells expressing different levels of *Terc-53* or the *Scramble* RNA. *Terc-53* levels were monitored by Northern blotting (top panels). 5S rRNA and  $\beta$ -actin were used as loading controls.

(C) Immunoblotting examination of Hmnr protein levels (bottom panels) in N2a cells expressing *Terc-53*, *Terc-53 Mut* that does not bind Hmnr, or the *Scramble* RNA. *Terc-53* and *Terc-53 Mut* levels were monitored by Northern blotting (top panels). 5S rRNA and  $\beta$ -actin were used as loading controls.

(D) Immunoblotting examination of Hmnr proteins in N2a cells expressing *Terc-53*, or the *Scramble* RNA, before and after Cycloheximide (a protein synthesis inhibitor) treatment.  $\beta$ -tubulin was used as a loading control.

(E) Immunoblotting examination of Hmnr proteins in N2a cells expressing *Terc-53*, or the *Scramble* RNA, before and after Chloroquine (a autophagy inhibitor) treatment.  $\beta$ -tubulin was used as a loading control.

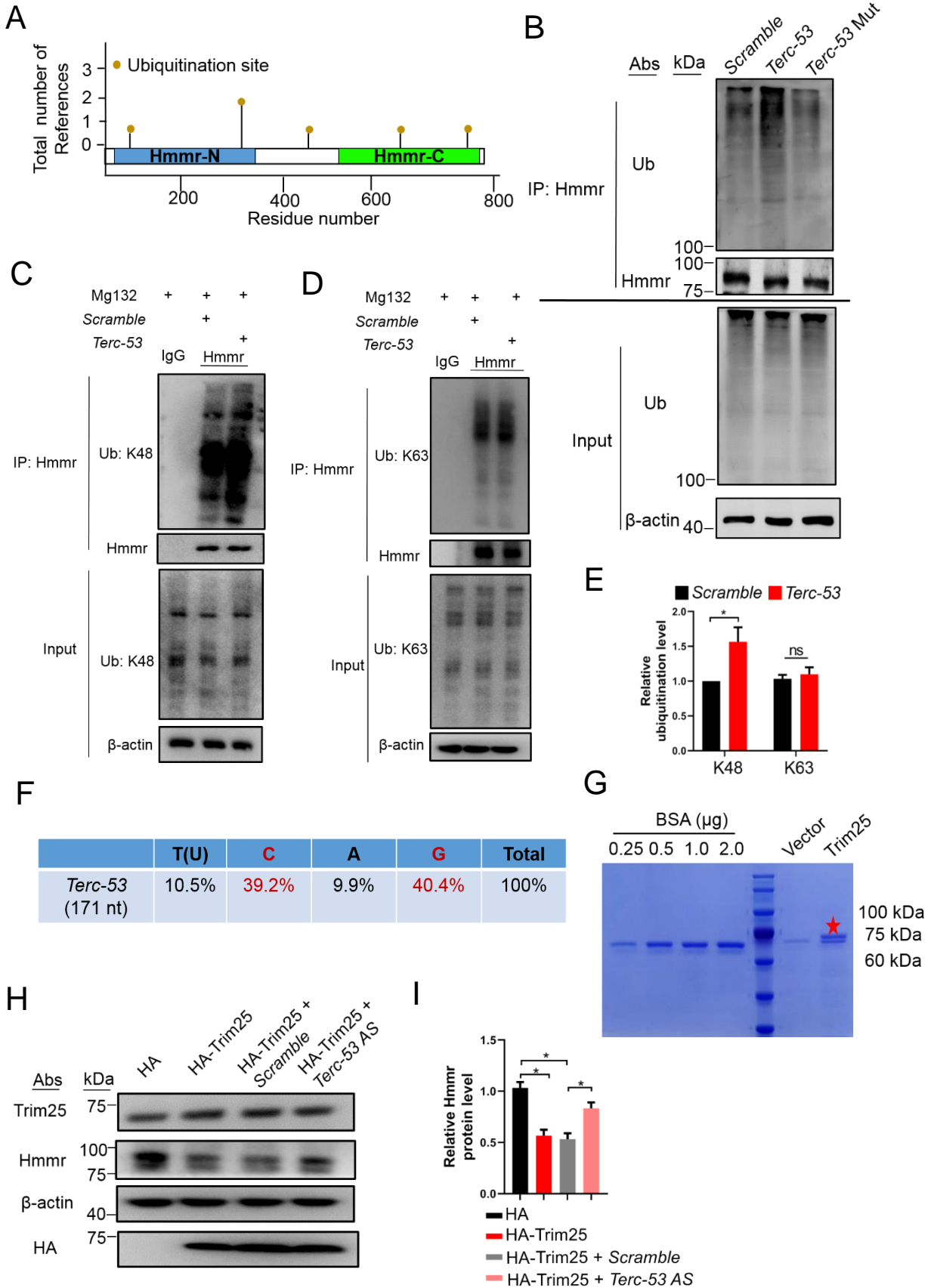


**Figure S13. Trim25 is the ubiquitin ligase for *Terc-53*-mediated Hmnr degradation.**

(A) The ubiquitination sites in Hmnr protein, predicted by PhosphoSitePlus.

(B) Endogenous Hmnr was immunoprecipitated from N2a cells stably expressing *Terc-53*, *Terc-53* Mut that does not bind Hmnr, or the *Scramble* RNA. The ubiquitination levels of the cell lysates (bottom) and the purified Hmnr (top) were examined by immunoblotting using a ubiquitin antibody.  $\beta$ -actin was used as a loading control for the cell lysate samples. The levels of purified Hmnr were monitored using a Hmnr antibody.

(C-D) Hmnr was immunoprecipitated from *Terc-53*-overexpressing (*Terc-53*) or the *Scramble* RNA-expressing (*Scramble*) N2a cells. The purified proteins were examined with an antibody specific for K48-linked (Ub: K48) (Panel G) or K63-linked (Ub: K63) (Panel H) polyubiquitin chains.

(E) Quantification of the relative ubiquitination levels in Panel C and D.

(F) GC content enrichment analysis of *Terc-53*.

(G) Coomassie staining of purified HA-Trim25 (indicated by the red star). The concentration of the purified protein was determined using BSA standards.

(H) Immunoblotting examination of Hmnr protein levels in N2a cells expressing *Terc-53* antisense RNA (*Terc-53 AS*) or the *Scramble* RNA in addition to overexpressing Trim25.

(I) Quantification of the relative Hmnr protein levels in Panel H (n = 3).

Data are presented as mean  $\pm$  SD. ns, no significance, \*p < 0.05, \*\*p < 0.01.



**Figure S14. Mutation of the ubiquitination sites on Hmnr stabilizes the protein.**

(A) HEK293T cells were co-transfected with HA-tagged Trim25, Flag-tagged ubiquitin, and Myc-tagged Hmnr. Cell lysates were subjected to immunoprecipitation and Mass spectrometry analysis to identify ubiquitination sites. The Hmnr peptides with a ubiquitination site were highlighted in red (upper panels). Lower panels: A schematic diagram showing the two evolutionarily conserved lysine residues (K265 and K736) for Hmnr ubiquitination, and the protein structure predict by Alphafold2.

(B) N2a cells expressing Myc-tagged wild-type Hmnr (Myc-Hmnr<sup>WT</sup>) or the K265R+K736R mutant (Myc-Hmnr<sup>2KR</sup>) were treated with cycloheximide (CHX) (a translation inhibitor) for the indicated periods of time. Lysates were subjected to immunoblotting analysis with Myc and  $\beta$ -actin antibodies (top panels). The bottom panel: quantification of the relative levels of Myc-Hmnr<sup>WT</sup> and Myc-Hmnr<sup>2KR</sup> with time (n = 3).

(C) N2a cells stably expressing *Terc-53* and *Terc-53 AS* or the *Scramble* RNA were transfected with Myc-Hmnr<sup>WT</sup> or Myc-Hmnr<sup>2KR</sup>. The expression levels of Myc-Hmnr<sup>WT</sup> or Myc-Hmnr<sup>2KR</sup> were examining by immunoblotting.

Data are presented as mean  $\pm$  SD. ns, no significance, \*p < 0.05, \*\*p < 0.01.

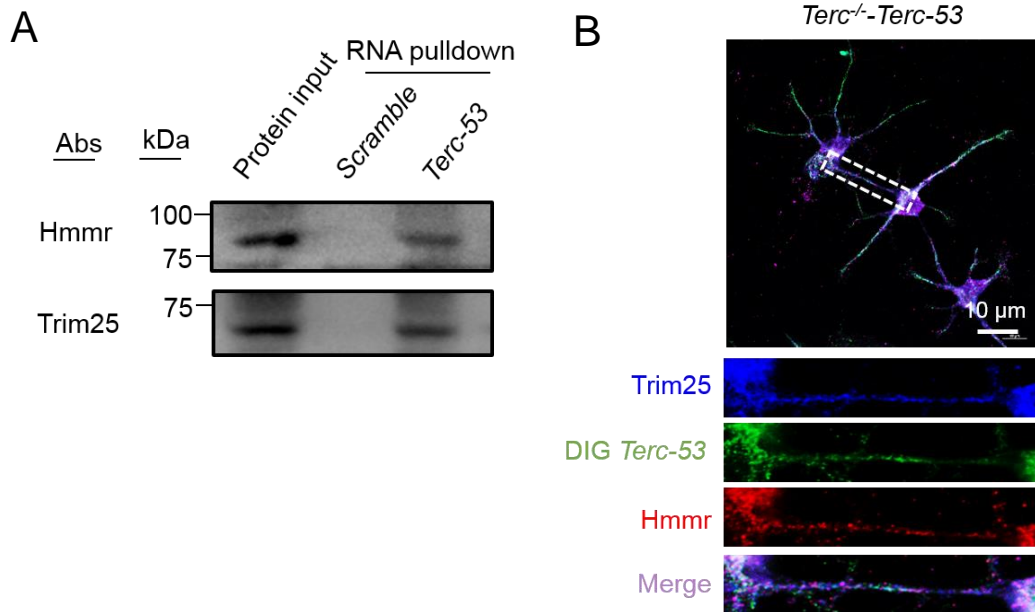
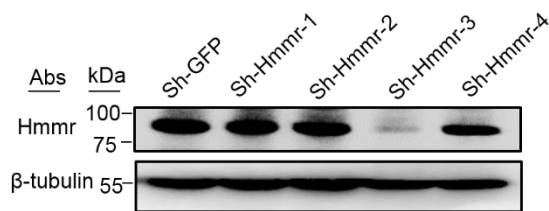


**Figure S15. Interaction of *Terc-53*, Hmnr and Trim25 in primary neurons.**

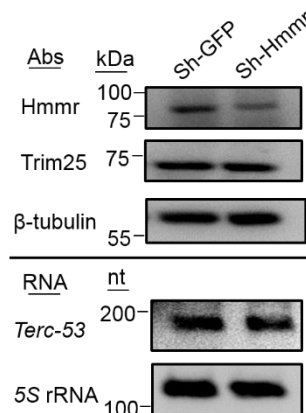
(A) Biotinylated *Terc-53* or the *Scramble* RNA were incubated with the lysate of 16-day DIV (days in vitro) *Terc<sup>-/-</sup>* primary neurons for the RNA pulldown assay, followed by immunoblotting of the indicated proteins.

(B) Representative images of *Terc-53* FISH, and Hmnr and Trim25 immunostaining in *Terc<sup>-/-</sup>* *Terc-53* primary neurons.

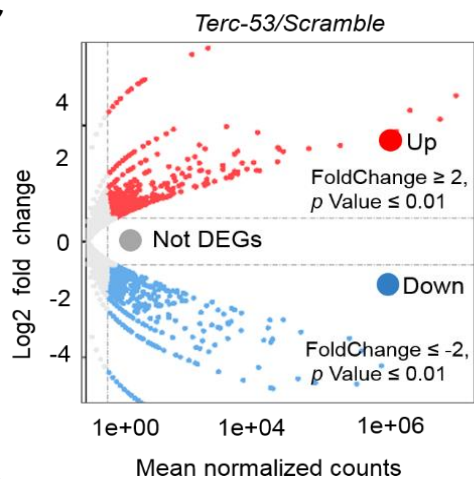
A



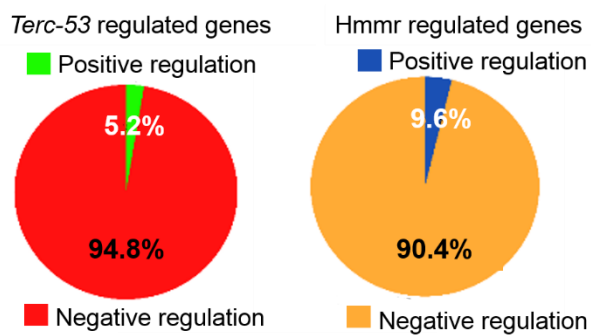
B



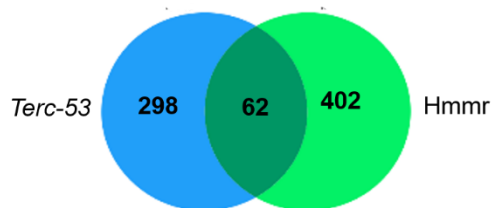
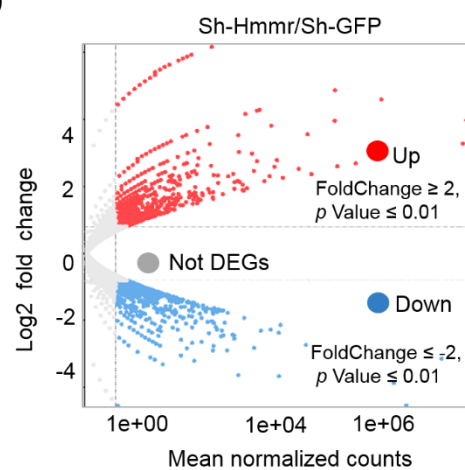
C



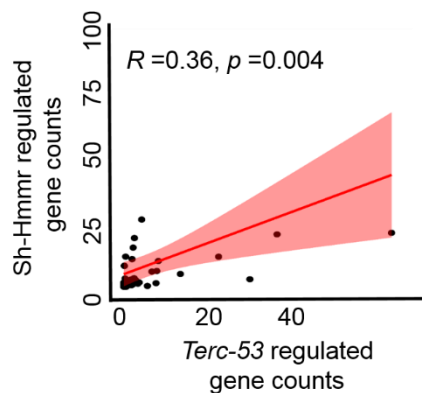
E



D



F



G

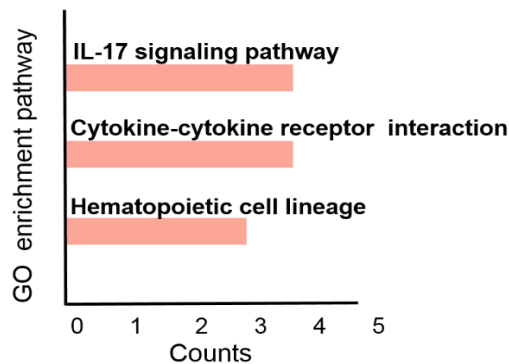


**Figure S16. RNA-seq analysis of *Terc-53*-overexpressing or *Hmmr*-knockdown N2a cells.**

(A) Immunoblotting examination of *Hmmr* protein levels in N2a cells with different shRNA constructs for *Hmmr* knockdown. A shRNA construct for GFP (sh-GFP) was used as a negative control.  $\beta$ -tubulin was used as a loading control.

(B) The levels of *Trim25* and *Terc-53* in N2a cells with (sh-*Hmmr*) or without (sh-GFP) *Hmmr* knockdown.

(C) Differentially expressed genes (DEGs) identified from comparison of the expression profile in *Terc-53*-overexpressing N2a cells and that in the *Scramble* RNA-expressing cells. Red dots represent upregulated DEGs. Blue dots represent downregulated DEGs. Gray dots represent non-DEGs.

(D) Differentially expressed genes (DEGs) identified from comparison of the expression profile of *Hmmr*-knockdown (sh-*Hmmr*) N2a cells and that of the control (sh-GFP) cells. Red dots represent upregulated DEGs. Blue dots represent downregulated DEGs. Gray dots represent non-DEGs.

(E) Venn diagram showing the overlap of transcripts from positively-regulated and negatively-regulated gene sets.

(F) Correlation analysis of differentially expressed genes in *Terc-53*-overexpressing or *Hmmr*-knockdown cells normalized to control. P values were calculated by Fisher's exact test.

(G) Gene ontology (GO) pathway analysis of genes co-regulated by *Terc-53* overexpression and *Hmmr* knockdown.

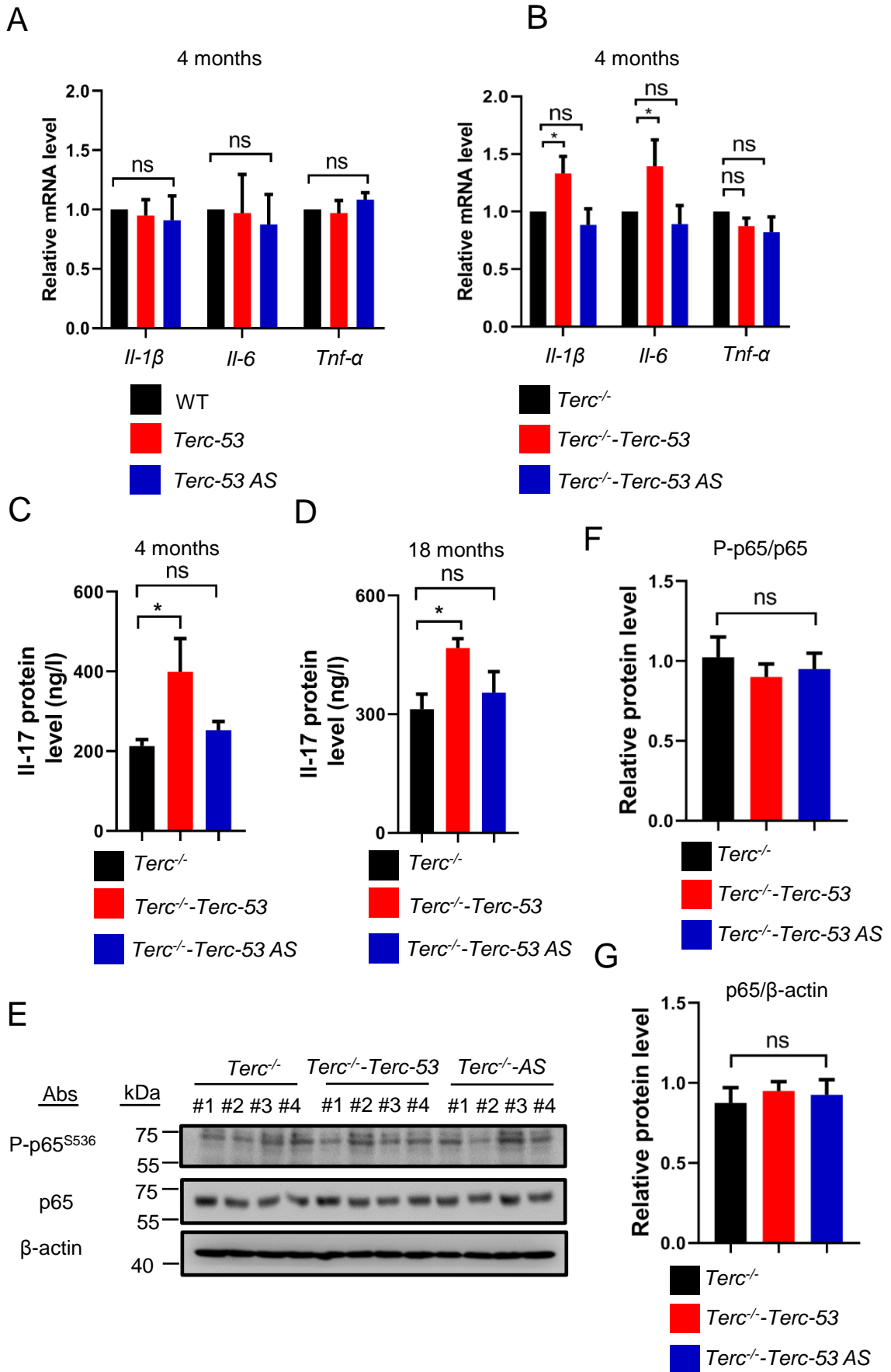


**Figure S17. The effects of *Terc-53* overexpression on pro-inflammatory factors.**

(A) RT-qPCR analysis of the levels of the mRNAs as indicated in the hippocampus of WT, *Terc-53* and *Terc-53 AS* male mice at 4 months of age (n = 4).

(B) RT-qPCR analysis of the levels of the mRNAs as indicated in the hippocampus of *Terc*<sup>-/-</sup>, *Terc*<sup>-/-</sup>-*Terc-53* and *Terc*<sup>-/-</sup>-*Terc-53 AS* male mice at 4 months of age (n = 4).

(C-D) Il-17 protein levels in the hippocampus of 4 months-old (Panel C) and 18-month-old (Panel D) *Terc*<sup>-/-</sup> and *Terc*<sup>-/-</sup>-*Terc-53* and *Terc*<sup>-/-</sup>-*Terc-53 AS* male mice as determined by ELISA (n = 3).

(E) Immunoblots of phospho-NF-κB p65 (Ser536) (P-p65<sup>S536</sup>) and p65 proteins in the hippocampus of *Terc*<sup>-/-</sup> and *Terc*<sup>-/-</sup>-*Terc-53* and *Terc*<sup>-/-</sup>-*Terc-53 AS* (*Terc*<sup>-/-</sup>-*AS*) male mice at 18 months of age. β-actin was used as a loading control.

(F-G) Quantification of the relative protein levels in Panel E (n = 4).

Data are presented as Mean ± SD. ns, no significance, \*p < 0.05, \*\*p < 0.01.